Electron Recombination Kinetics of Dye-Sensitized Solar Cells based on TiO_2 Nanorod Arrays Sensitized with Different Dyes

Hongxia Wang,[*1] *Meinan Liu,*[*1] *Min Zhang,*[2] *Peng Wang,*[2] *Hidetoshi Miura,*[3] *Yan Cheng*[1] *and John Bell*[1]

[1] School of Engineering System, Queensland University of Technology, 2 George Street, Brisbane, QLD 4001, Australia

[2] State Key Laboratory of Polymer Physics and Chemistry, Changchun Institute of Applied Chemistry, Chinese Academy of Sciences, Changchun, 130022, China

[3] Chemicrea Inc., Tsukuba Centre, 2-1-6, Sengen, Tsukuba Ibaraki, 305-0047, Japan

*Corresponding Authors:

Hongxia Wang, Tel: +61 7 3138 1984, Fax: +61 7 3138 9965, Email: hx.wang@qut.edu.au

and Meinan Liu, Meinan.liu@qut.edu.au.

ABSTRACT The performance and electron recombination kinetics of dye-sensitized solar cells based on TiO_2 films consisting of one-dimensional nanorod arrays (NR-DSSCs) which are sensitized with dye N719, C218 and D205 respectively have been studied. It has been found that the best efficiency is obtained with the dye C218 based NR-DSSCs, benefiting from a 40% higher short-circuit photocurrent density. However, the open circuit photovoltage of the N719 based cell is 40 mV higher than that of the organic dye C218 and D205 based devices. Investigation of the electron recombination kinetics of the NR-DSSCs has revealed that the effective electron lifetime, τ_n, of the N719 based NR-DSSC is the lowest whereas the τ_n of the C218 based NR-DSSC is the highest among the three dyes. The higher V_{oc} with the N719 based NR-DSSC is originated from the more negative energy level of the conduction band of the TiO_2 film. In addition, in comparison to the DSSCs with conventional nanocrystalline particles based TiO_2 films, the NR-DSSCs have shown over two orders of magnitude higher τ_n when employing N719 as the sensitizer. Nevertheless, the τ_n of the DSSCs with the C218 based nanorod arrays is only ten-fold higher than the that of the nanoparticles based devices. The remarkable characteristic of the dye C218 in suppressing the electron recombination of DSSCs is discussed.

KEYWORDS: TiO_2 nanorod arrays, dye-sensitized solar cells, electron lifetime, dye N719, dye C218, photovoltage decay, impedance spectroscopy

Developing clean, renewable energy resources to satisfy the increasing demand for energy by our society has become one of the most important global issues to be solved in this century. Generation of energy from solar radiation via photovoltaic technology is considered as one of the promising solutions for this world-wide issue. Owing to their promise of low cost of readily available materials, ease of fabrication and good performance, dye-sensitized solar cells (DSSCs) have attracted great attention in the past two decades.[1-4] A typical DSSC consists of a photoanode made of a dye coated mesoporous TiO_2 film, an electrolyte containing I^-/I_3^- redox couple and a platinum counter electrode. The device operates following a cascade of physicochemical processes involving photon-induced electron generation by the dye, electron transfer from the dye molecule to the TiO_2 particle followed by electron transport in the TiO_2 film before being collected by external circuit.[5] Besides the above processes, electron at the conduction band of TiO_2 can also recombine with I_3^- in the electrolyte, leading to the reduced performance of DSSCs. Therefore, the performance of DSSCs is actually determined by the competition between the desired processes of forward electron injection and transport and the unwanted backward electron recombination.[6]

Electron transport in TiO_2 films is generally described by a multiple trapping/detrapping process where the electron in the conduction band falls in the shallow traps and then thermally detrapped from the sub-bandgap states to the conduction band. The electron trapping/detrapping process determines the effective electron lifetime, τ_n, and effective electron diffusion coefficient, D_n.[7-10] It has been demonstrated that the microstructure (e.g. crystal structure, morphology, *etc*.) of the TiO_2 film has a profound impact on both τ_n and D_n of DSSCs.[11-16] The D_n of DSSCs based on conventional mesoporous TiO_2 films consisting of an interconnected nanoparticle network is 2-3 orders of magnitude lower than that of bulk material owing to the large amount of grain boundaries and defects.[8, 17, 18] To solve this problem, one-dimensional (1D) structured nano-materials such as nanowires, nanorods, nanotubes have been developed as a more efficient electron transport medium for DSSCs. Indeed, improved conversion efficiency with TiO_2 nanorods based DSSCs has been reported by Adachi *et al* and Kang *et al* even though the nanowires and nanorods were randomly distributed in the TiO_2 films used in their work.[12, 19] TiO_2 films consisting of vertically aligned 1D-nanostructures are expected to be superior than the films consisting of randomly connected 1D materials owing to the shorter mean electron transport pathway, leading to a lower recombination and a higher charge collection efficiency.

Methods for the preparation of 1D TiO_2 nanotubes which grow vertically on Ti foil have been developed.[20] The kinetics study of electron transport and recombination of the 1D nanotube array based DSSCs has shown that the electron diffusion length, L_n, was around 100 μm and the electron collection efficiency was nearly unity for a 20 μm-thick film.[21] Zhu *et al* have reported that, compared to the nanoparticulates based film, the τ_n of the nanotube film was one order of magnitude higher. However, the D_n of the two types of films was comparable. As a result, the electron diffusion length of the nanotubes based film was around 3-fold higher than that of the nanoparticle film, leading to a higher electron collection efficiency. [22] However, the 1D nanotube array based films have drawbacks which may limit their applications in DSSCs in practice. Firstly, illumination has to go across the counter electrode before reaching the photoactive electrode of the DSSCs because the photoanode (Ti foil) is not transparent. Consequently, significant light loss will occur due to the light absorption of the counter electrode and the iodine-based electrolyte. Secondly, compared to the DSSC which is illuminated from the front of the photoanode, the average path which the electron has to travel before being collected by external circuit is longer for a counter electrode illumination mode. Therefore, the electron collection efficiency and the conversion efficiency of the device will be reduced if the electron diffusion length is a performance limiting factor.

Recently, a one-step hydrothermal method has been developed to grow 1D TiO_2 nanowire/nanorod arrays on a transparent fluorine doped tin oxide (FTO) substrate directly.[23-25] The simplicity of the method offers the possibility for fabrication of high efficiency DSSCs with the ordered 1D array films. Our previous work has confirmed that there is a thin compact TiO_2 layer underneath the nanorod array, which can effectively eliminate the electron recombination reaction with I_3^- at FTO/electrolyte interface of the DSSCs.[25] This unique feature allows us to investigate the kinetics of electron recombination of the corresponding DSSCs directly by dynamic methods such as photovoltage decay and electrochemical impedance spectroscopy (EIS). Recently Bang *et al* have investigated the performance of the TiO_2 nanorod arrays in quantum dot CdSe based photoelectrochemical cells. They observed a longer effective electron lifetime with the nanorod arrays compared to the nanoparticle counterpart.[26] However, high efficiency DSSCs normally use dyes with carboxyl ligand (-COOH) through which the dye can firmly anchor on the TiO_2 film. Besides ruthenium complex based dyes (e.g. N719), organic dyes such as D205 and C218 which possess high light extinction coefficient have recently been developed to improve the

efficiency of DSSCs.[27] Although the kinetics of electron recombination of these dyes have been investigated in conventional anatase nanocrystalline mesoporous TiO_2 film, such study has not been reported in the 1D nanorod arrays however. Moreoever, it has been reported that the dye adsorption on the TiO_2 film is affected by both the crystal structure and morphology of the TiO_2 particles.[28] Therefore, it will be interesting to know how the kinetics of electron recombination in the rutile nanorod arrays varies when sensitized with these organic dyes compared to the ruthenium complex. Such study will provide useful information for optimization of the design of new dyes for DSSCs with improved performance. In this work, the three dyes N719, D205 and C218 (the molecule structures are shown in Figure 1) are incorporated in the nanorod array system (NR-DSSCs). The variation of the TiO_2 conduction band and the effective electron lifetime of the NR-DSSCs with the three dyes have been studied comprehensively. Moreover, the electron recombination kinetics of the NR-DSSCs is also compared to that of the DSSCs with conventional TiO_2 nanoparticles based films. In the following section, we use NR-X (X= N719, C218 or D205) to name the DSSCs with the different dye coated nanorod arrays and NP-X for the cells with the different dye coated nanoparticles based films for clarity.

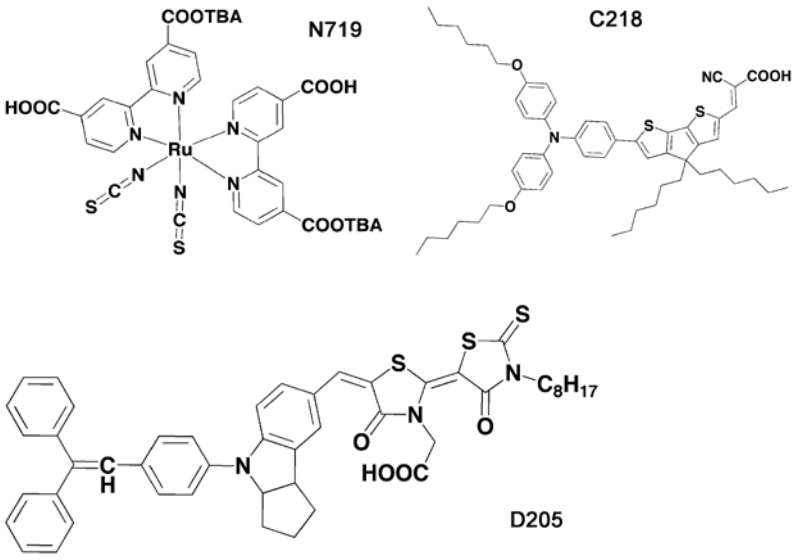

Figure 1. Molecule structures of the dyes investigated

EXPERIMENTAL SECTION

Synthesis of TiO_2 nanorod-array

A cleaned fluorine doped tin oxide (FTO) glass substrate (Hartford glass, TEC15) was placed into an autoclave (45 ml, Parr Instrument) which contained a precursor solution consisting of titanium butoxide (3.0 mM) and concentrated hydrochloric

acid (32 wt%) in de-ionized water (HCl: H_2O = 1:2, v/v). The autoclave was placed in an electric oven at 160 ^oC for 12 h to grow the nanorod array. After cooling down to room temperature, the TiO_2 coated FTO substrate was taken out and then thoroughly washed with distilled water. The film was dried in air at ambient temperature and sintered at 500 ^oC on a hotplate for 30 mins. The TiO_2 film was subjected to a $TiCl_4$ treatment (40 mM aqueous solution) at 70 ^oC for half an hour. After being washed with distilled water, the $TiCl_4$ treated film was then sintered at 450 ^oC for 30 mins on a hotplate in air. The TiO_2 films when they were still warm (80 ^oC) were respectively immersed in the dye bath containing N719 (0.25 mM, Solaronix), C218 (0.1 mM) or D205 (0.25 mM) in a solvent mixture of acetonitrile / tert-butanol (1:1, v/v) for 16 h. Co-adsorbent 3α-7α-dihydroxy-5β-cholic acid (1mM) was added in the dye solution C218 or D205 to reduce the dye aggregation on the TiO_2 films.

Assembly of dye-sensitized solar cells

DSSC was fabricated by sealing the dye coated TiO_2 electrode with a thermally platinized FTO counter electrode together by a Surlyn film (25 μm, Solaronix). The electrolyte composed of 0.6 M 1-propyl-3-methylimidiazolium iodide, 0.05 M I_2, 0.1 M guanidinium thiocyanate, 0.2 M NaI, 0.1M N-methyl benzimidiazium in 3-methoxypropionitrile was introduced into the DSSC through the holes predrilled in the counter electrode, which were then sealed with a Surlyn film together with a microscope glass slip. For comparison, reference DSSCs based on nanocrystalline TiO_2 particle based films made from a commercial paste (DSL-18-NR, Dyesol) were also assembled by following the procedure which has been reported in our previous work.[29] The FTO substrate was coated with a compact layer of TiO_2 by spray pyrolysis before being deposited the nanoparticle film. The same dye and electrolyte material were used in the reference cells unless otherwise stated. The thickness of the TiO_2 nanocrystalline particles based film was 13 μm. The active area of all the DSSCs was 0.25 cm^2.

Characterizations

The absorbance of the dye N719, C218 and D205 at different concentration were measured by a UV-visible spectrophotometer (Cary 50). The dye uploading in the TiO_2 films was determined in the following method. For the dye N719, the dye was desorbed from the TiO_2 film by immersing the film in a 1M NaOH aqueous solution, and the amount of the dye in the aqueous solution was then determined through a calibrated relationship of Absorbance *vs* Concentration of the dye solution. Since both the dye C218 and D205 do not dissolve in the NaOH aqueous solution, the dye uploading in the TiO_2 films was determined by measuring the change of the concentration of the original dye bath (D205 or C218) after the dye adsorption process was completed. The light extinction coefficient of the three dyes was calculated according to Beer-Lambert law.

The morphology and crystal structure of the hydrothermally prepared TiO_2 films were investigated by scanning electron microscope (SEM, Quanta 200) and powder X-ray diffraction (XRD, PANanalytical Xpert Pro), respectively. The thickness of the as-obtained films was also measured by atomic force microscopy (AFM, Xe-100, PASI). The photocurrent density-voltage (J-V) characteristics of the DSSCs was evaluated using a Xe lamp (150 W) based solar simulator system (Newport) by recording the current of the cells as a function of applied bias under an AM1.5 illumination (100 mW/cm^2). The illumination intensity of the solar simulator was measured with a calibrated silicon photodiode.

The photovoltage decay measurement of the DSSCs was performed under open circuit condition using a Versa-stat 3 electrochemical workstation (Princeton Applied Research) and a high intensity light emitting diode (LED, 627 nm). The DSSCs were illuminated until a photostationary state was reached, after which the LED was switched off and the photovoltage transient was recorded.

The electrochemical impedance spectroscopy (EIS) of the DSSCs was measured using the same equipments in the frequency range of 50,000 – 0.1 Hz at room temperature. The EIS measurement was carried out under illumination at open-circuit

condition as well. The EIS spectra were analysed by a Zview software using a transmission line equivalent circuit. [29, 30] to obtain the information of chemical capacitance, electron recombination resistance and electron transport resistance of the DSSCs.

RESULTS AND DISCUSSION

Hydrothermally prepared TiO_2 nanorod array film

The SEM pictures of the hydrothermally prepared TiO_2 film coated on FTO substrate are shown in Figure 2(a, b). As can be seen, the nanorods are vertically grown on the substrate. The average diameter of the nanorod is around 80 nm which is similar to that reported by Liu *et al*,[23] but much larger than the results reported by Feng *et al* (10-35 nm).[24] Both SEM (Figure 2(b)) and AFM results (Figure 2(c)) show that the average length of the nanorod (film thickness) is about 500 nm which is much shorter than the length reported by Liu *et al* (2 μm) and by Feng *et al* (4 μm) as well.[23, 24] Though both Liu *et al* and Feng *et al* have observed an increased length of the nanrods by extending the reaction time, the length of the nanorods did not change beyond 12 h in our case.

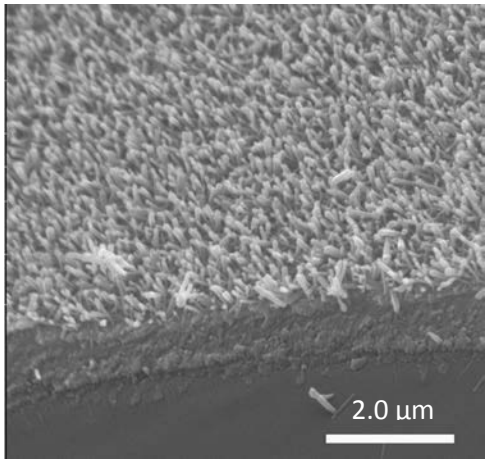

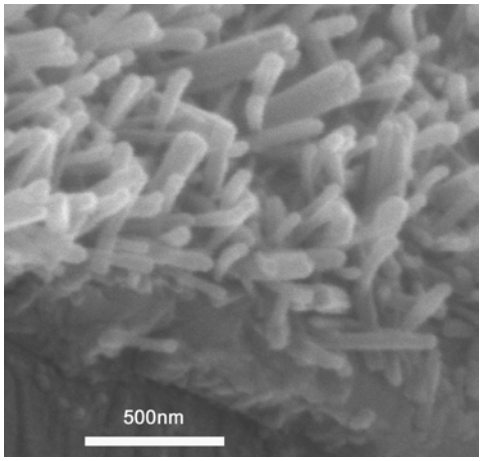

(a) **(b)**

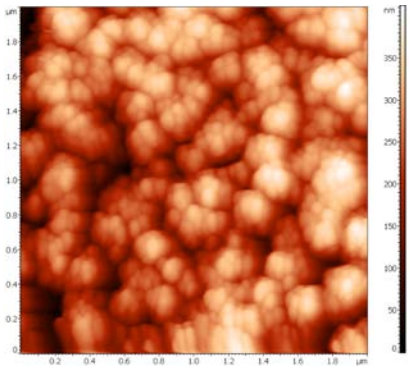

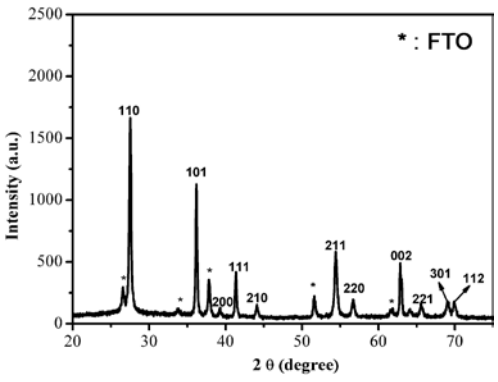

(c) **(d)**

Figure 2. Images of SEM (a, b) and AFM (c) as well as XRD result (d) of the hydrothermally prepared TiO_2 film grown on a FTO substrate. The XRD peaks labelled by asterisk are from the FTO substrate.

The XRD pattern (Figure 2(d)) of the TiO_2 film with the nanrod array shows that, except the diffraction peaks from the FTO substrate, all the rest of the peaks are attributed to the tetragonal rutile phases of TiO_2 (SG, $P4_2/mnm$, JCPDS card No. 21-1276, $a = b = 0.459$ nm, $c = 0.2959$ nm). Moreover, the nanorod array does not show preferential orientation, which differs from the results reported by Liu *et al* and Feng *et al* as well. These differences are probably caused by the different experimental conditions for materials synthesis.

Photovoltaic performance of dye-sensitized solar cells based on the nanorod arrays

The characteristics of photocurrent density (J)-voltage (V) of the NR-N719, NR-D205 and NR-C218 are shown in Figure 3(a). The first striking feature is that the NR-C218 produces much higher short circuit photocurrent density (J_{sc}) than the NR-N719 and the NR-D205. The J_{sc} of the NR-C218 is 2.43 mA/cm^2, which is around 40% higher than the J_{sc} of the other cells (J_{sc} =1.73 mA/cm^2 for NR-N719; and J_{sc} =1.71 mA/cm^2 for NR-205). On the other hand, the open-circuit voltage (V_{oc}), which is another important parameter determining the performance of DSSCs, shows the trend of NR-N719 > NR-C218 ≈ NR-D205. The V_{oc} of the NR-N719 is 804 mV, which is 40 mV higher than that of the NR-C218 and NR-D205. In spite of the higher V_{oc} for the NR-N719, the highest efficiency (efficiency =1.51%) is obtained with the NR-C218 benefiting from the significantly higher J_{sc}. Given the fact that the thickness of the nanorod array film is only about 500 nm, the performance of the device is quite impressive.

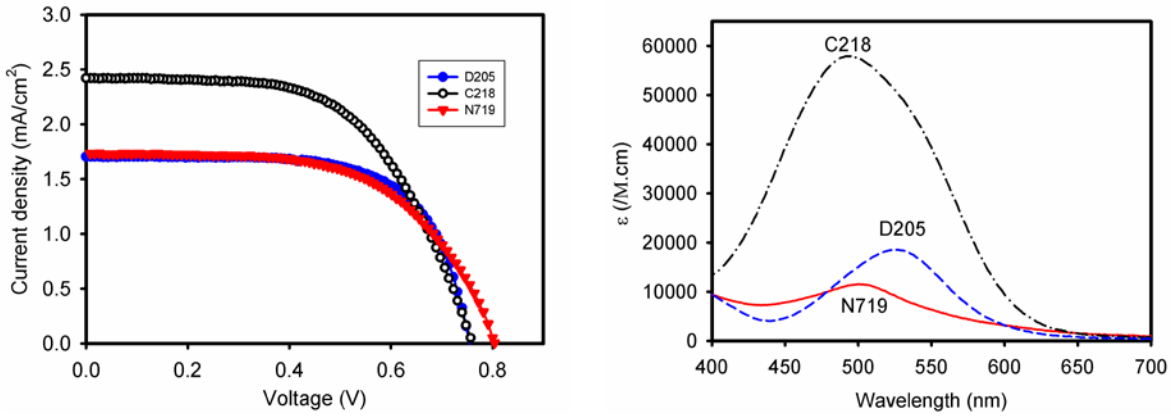

(a) (b)

Figure 3. (a) Photocurrent density-voltage plot of the dye-sensitized solar cells with TiO_2 nanorod arrays sensitized with dye N719, D205 and C218 respectively and (b) the light extinction coefficient of the three dyes used in this work

The J_{sc} of a DSSC is determined by the synergistic effect of photon-induced electron generation of the dye material (light harvesting efficiency), efficiency of electron injection from the dye excited state to the conduction band of TiO_2 and the

electron collection efficiency by external circuit. It is known that the electron collection efficiency is determined by the effective electron diffusion length, L_n, in relative to the thickness, d, of the TiO_2 film. When L_n is much higher than d (e.g. $L_n/d > 3$), the electron collection efficiency is close to 100%.[31] As shown in the later section, the ratio of L_n/d for all the DSSCs is more than 3, therefore the J_{sc} should be controlled by either the electron injection efficiency and/or the light harvesting efficiency. Previous extensive studies have shown that the electron injection efficiency is controlled by the energy offset between the dye excited state and the conduction band of TiO_2.[2] The conduction band of a rutile phase TiO_2 material is around -0.3 eV *vs* NHE,[32] therefore the energy driving force for the electron injection is 0.35 eV for N719 (the energy level of the excited state of N719 is -0.65 eV *vs* NHE) [2], which is sufficient for an efficient electron injection.[2] Though the data for the energy level of the excited state of D205 and C218 are not available yet, theoretical calculations have shown that the driving force for electron injection is around 0.5 eV for D205 and over 0.9 eV for C218. [33,34] Obviously, the electron injection efficiency should not be the reason for the different J_{sc} either. Therefore, the light harvesting efficiency should be responsible for the different J_{sc}. The light harvesting efficiency depends on the light extinction coefficient of the dye and the amount of dye which adsorbs on the TiO_2 film. The maximum light extinction coefficient, ε, of the three dyes used in this work is shown in Figure 3(b). Apparently, the dye C218 has much stronger light absorption capability with $\varepsilon = 5.6 \times 10^4\ M^{-1}\ cm^{-1}$ at 525 nm, which is around five-fold that of N719 ($\varepsilon = 1.13 \times 10^4\ M^{-1}\ cm^{-1}$ at 500 nm in 1 M NaOH aqueous solution) and three-fold that of D205 ($\varepsilon = 1.87 \times 10^4\ M^{-1}\ cm^{-1}$ at 526 nm). The coverage of the three dyes on the TiO_2 nanorod arrays is 1.06×10^{-9} mol/ cm^2 for N719, 1.37×10^{-9} mol/ cm^2 for C218 and 1.7×10^{-9} mol/ cm^2 for D205 respectively. As a consequence, the light harvesting efficient of the dye coated TiO_2 films have the trend of C218 > D205 > N719, consistent with the variation of the J_{sc}.

Compared to organic dyes, ruthenium-complex dye such as N719 based DSSCs usually generates higher V_{oc}. This phenomenon is usually attributed to the lower electron recombination in the DSSCs with the ruthenium dye.[35] V_{oc} of a DSSC is the potential difference between the quasi-Fermi energy level of TiO_2 film under illumination and the redox level of I^-/I_3^- in the electrolyte. Theoretically, V_{oc} depends on the parameters of incident illumination intensity, I_{inj}, the concentration of free electron in the conduction band of TiO_2, n_{cb}, and the recombination reaction rate of free electron with oxidized species such as I_3^- in the device, k_{br}, as well as the concentration of I_3^- in the electrolyte, $[I_3^-]$ by $V_{oc} = \frac{k_B T}{q} In(\frac{I_{inj}}{n_{cb} k_{br} [I_3^-]})$. [5, 36]

Given a constant illumination intensity and the same electrolyte used for all the DSSCs, the variation of V_{oc} therefore should be determined by n_{cb} and/or k_{br}. In order to disclose the factor which is mainly responsible for the different V_{oc}, the density of chemical capacitance, C_μ, which accounts for the density of charges in the TiO_2 film is investigated (Figure 4).[37] It is found that the C_μ of NR-C218 is higher (up to 30%) than that of NR-D205 and NR-N719. The C_μ of the NR-D205 and the NR-N719 is comparable although their V_{oc} is different. It suggests that the difference in n_{cb} cannot account for the variation in V_{oc} of the DSSCs. Instead, the different V_{oc} is probably caused by the different electron recombination in the DSSCs.

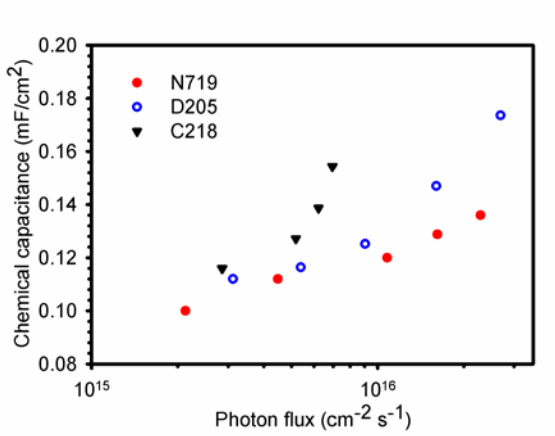

Figure 4. Chemical capacitance *vs* photon flux of the nanorod array based dye-sensitized solar cells sensitized with different dyes

Electron recombination kinetics of DSSCs with nanorod arrays

The techniques of open-circuit photovoltage decay and electrochemical impedance spectroscopy (EIS) are employed to investigate the electron recombination in the DSSCs. Figure 5(a) shows the plots of open-circuit photovoltage decay of NR-N719, NR-C218 and NR-D205 as a function of elapsed time in dark. Clearly, after the light is switched off, there is still substantial concentration of charges (as evidenced by the voltage) in the cells even after 200 seconds in dark. This suggests that the compact layer underneath the nanorod array can efficiently prevent the electron recombination reaction occurring at the FTO/electrolyte interface.[38] Therefore, the main pathway where electron in the TiO_2 film is scavenged is *via* back reaction with I_3^- in the electrolyte. The effective electron lifetime, τ_n, of the DSSCs at different voltage can therefore be determined by fitting the photovoltage decay plot according to Eq. 1.[39]

$$\tau_n = -\frac{k_B T}{q}\left(\frac{dV_{oc}}{dt}\right)^{-1} \qquad \text{(Eq.1)}$$

Where k_B is Boltzmann's constant, T is absolute temperature, q is elementary charge and t is elapsed time.

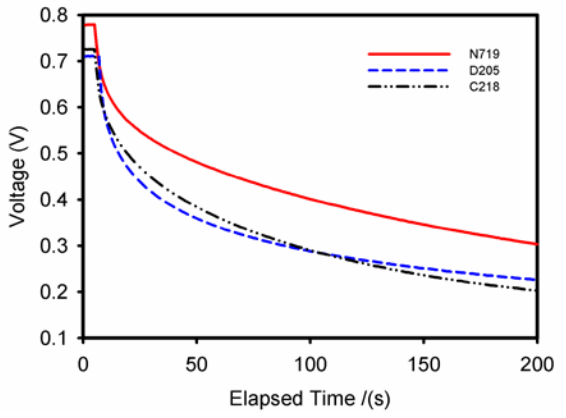

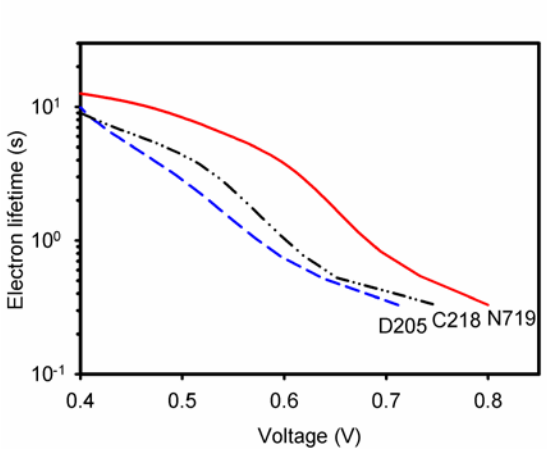

(a) (b)

Figure 5. (a) Open circuit photovoltage decay and (b) effective electron lifetime as a function of voltage of the DSSCs with the TiO_2 nanorod arrays sensitized with different dye materials

Figure 5(b) illustrates the τ_n of NR-N719, NR-C218 and NR-D205 as a function of voltage. τ_n shows the trend of NR-N719 > NR-C218 > NR-D205 over the voltage range investigated. At V = 0.6 V, τ_n of the NR-N719 is up to three times higher than that of NR-C218 and four times higher than that of NR-D205 respectively. This is consistent with the change of the V_{oc} of the cells shown in Figure 3(a). The variation of τ_n of the DSSCs is further confirmed by the EIS measurement (Figure 6(a)). Since the EIS technique for characterization of DSSCs is based on fitting the measured results with a transmission line based equivalent circuit, a reliable fitting is normally achieved in the voltage range when both the electron transport resistance and electron recombination resistance are substantial, which limits the availability of the data. [29] Only the EIS results from satisfactory fittings are used in this work.

Although both photovoltage decay and EIS data have suggested that NR-N719 has a lower electron recombination rate, it is worth to note that τ_n of a DSSC is determined by the distribution of the density of electron in the conduction band (free electron) and in the trap states (trapped electron) of the TiO_2 film. As a result, the τ_n is affected by the energy level of the conduction band of the TiO_2. The results shown in Figure 5(b) and Figure 6(a) which employ voltage as the reference for τ_n is a combined effect of the electron recombination and the variation of TiO_2 conduction band. However, the shift of TiO_2 conduction band caused by the dipole moments and the adsorption mode of dye molecules has been reported previously.[7, 40, 41] In order to find out whether the conduction band of the TiO_2 nanorod array is affected by the adsorption of the three different dyes, the chemical capacitance, C_μ, of NR-N719, NR-C218 and NR-D205 is compared in Figure 6(b). It is observed that the same C_μ is obtained for the organic dye D205 and C218 based cell at the same voltage. In contrast, the voltage of NR-N719 is much higher in order to produce the equivalent C_μ. It indicates that the conduction band energy level of the TiO_2 film in NR-N719 is more negative than that of the nanorod arrays in NR-D205 and NR-C218. Hence, it is more appropriate to use C_μ as the reference for the comparison of τ_n (Figure 6(c)) so as to exclude the influence of different conduction band energy levels on τ_n. It is found that, opposite to the widely assumption that ruthenium complex dyes have lower electron recombination than organic dyes in DSSCs,[35] τ_n

of NR-N719 is lower than that of NR-C218 and NR-D205. Therefore, the higher V_{oc} of the NR-N719 should be attributed to the higher conduction band energy level of the TiO_2 film. Similar phenomenon has also been observed by Li *et al*. In their work, the C218 based DSSCs showed higher electron lifetime and lower conduction band edge compared to the cell with the ruthenium complex Z907.[34] It is probably due to the different adsorption mode of the dyes on the TiO_2 film. Compared to the ruthenium complex, the dye molecule of C218 (Figure 1) has two aliphatic chains which are tethered to the conjugated backbone. When grafting on the surface of TiO_2, the two aliphatic chain can lead to more uncovered TiO_2 surface after dye-coating, which could subsequently interact with additive in the electrolyte such as guanidinium thiocyanate, leading to a compact layer consisting of the dye C218 and the electrolyte components. As a consequence, the surface states of the TiO_2 film would be reduced, resulting in a longer effective electron lifetime.[34] Moreover, the higher electron recombination with the NR-N719 could be related with the higher number of carboxyl group as well. Clifford *et al* has reported that the electron recombination of the dye with less number of carboxyl ligand is lower. [42] Since N719 has two -COOH groups while C218 or D205 has only one –COOH group, the extra carboxyl ligand might contribute to the increased electron recombination in the NR-N719. We have calculated the electron diffusion length, L_n of the nanorod arrays based DSSCs according to the EIS results. The ratio of L_n to the thickness of the nanorod array, *d* (L_n/d), which determines the electron collection efficiency of DSSCs, is more than 3 (Figure 6(d)) for all the DSSCs. Therefore, a higher electron collection efficiency is expected with those devices.

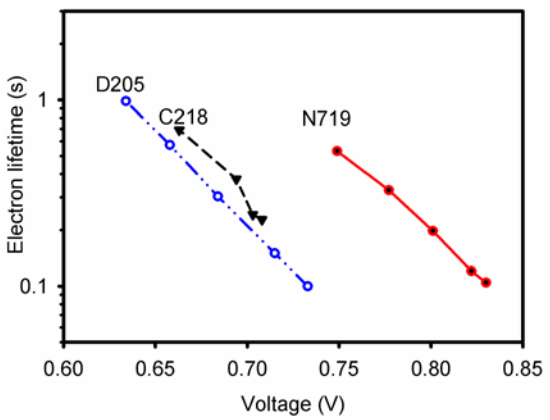

(a)

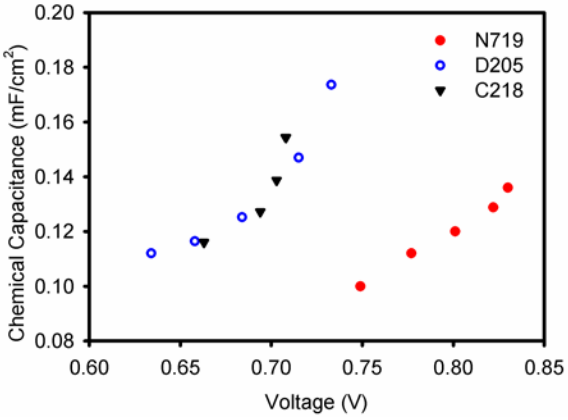

(b)

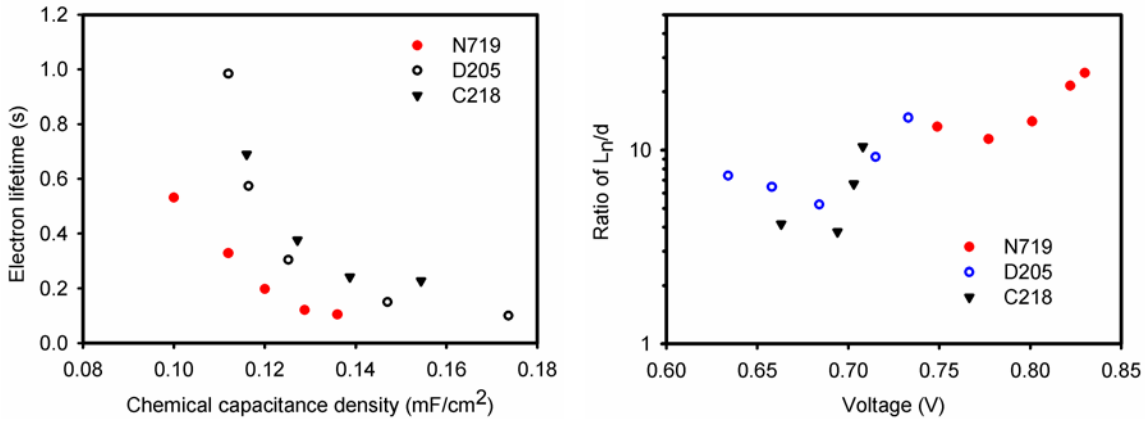

(c) **(d)**

Figure 6. Effective electron lifetime (a) and chemical capacitance (b) as a function of open circuit voltage, and effective electron lifetime versus chemical capacitance (c) and ratio of the electron diffusion length L_n to the thickness of TiO_2 nanorod array, d (L_n/d) (d) of the DSSCs based on the nanorod arrays sensitized with different dyes.

Effective electron lifetime of DSSCs with nanorod array and nanoparticle based TiO_2 films

Figure 7(a,b) shows the τ_n of the nanorod array and the nanoparticle based TiO_2 films which are sensitized with N719 or C218 respectively. It is observed that the τ_n of the nanorod array based film is more than one order of magnitude higher than that of the nanoparticle counterpart at a constant voltage (Figure 7(a)) in the case of using the dye N719 as sensitizer. The high electron recombination of the nanoparticle based film is probably due to the higher density of surface states. It is generally accepted that the number of surface states is proportional to the surface area of TiO_2 film. The surface areas of the TiO_2 nanorod arrays is around 20 m^2/g, which is much lower than the film consisting of the nanoparticles with size around 20 nm. Moreover, the thickness of the nanoparticles based film (13 μm) is much higher compared to the nanorod arrays (500 nm), therefore the former should have a much higher density of surface states, leading to a higher electron recombination.[43] However, the effect of the nanorod array on enhancing τ_n is less pronounced when using the dye C218. The τ_n of NR-C218 is no more than 2-fold that of NP-C218 (Figure 7(b)).

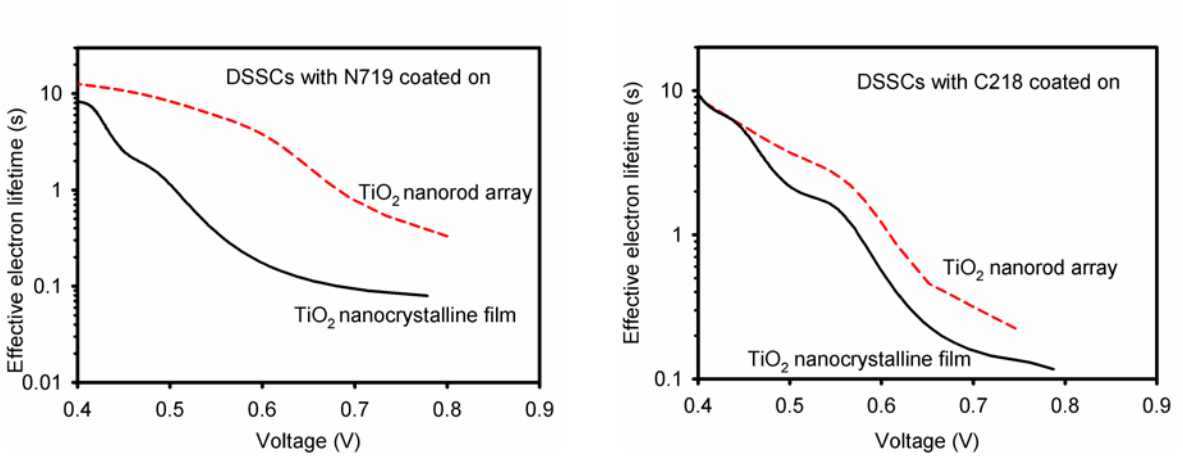

(a) **(b)**

Figure 7. Effective electron lifetime of the dye-sensitized solar cells with nanorod arrays and nanoparticles based TiO_2 film coated with the dye N719 (a) and C218 (b).

As discussed above, such behaviour of τ_n can also be due to the different energy level of the conduction band edge of TiO_2 film when using voltage as the reference. The TiO_2 nanorod array is rutile phase, the conduction band of which is around 0.2 eV lower than the anatase phase based nanoparticle films. Therefore, it is necessary to use density of charge as the reference for the comparison of τ_n. As shown in Figure 8, the NR-DSSCs (solid symbols) have higher electron lifetime than the NP-DSSCs (empty symbols) for both dyes. This solid evidence demonstrates that the 1D nanostructure does help reduce the electron recombination compared to the film consisting of randomly packed nanoparticle network. Nevertheless, the effect of the nanorod array on enhancing τ_n relative to the nanoparticle film is still more significant with the N719 dye compared to the C218 dye. The τ_n of the NR-N719 is around two orders of magnitude higher than that of the NP-N719 whereas the NR-C218 is only around one order of magnitude higher than the NP-C218. This huge difference is ascribed to the much higher coverage of the dye C218 on the nanoparticles based TiO_2 film owing to its much higher surface area, which enhances the benefiting effect of C218 on reducing the electron recombination in the device. This assumption is supported by the observation that the NP-C218 produces similar V_{oc} with the NP-N719 (Figure S1) in the *J*-V characteristic plot, which suggests that the lower conduction band edge of the TiO_2 films coated with the dye C218 can be fully compensated by the reduced electron recombination at a higher dye uploading. It is worthwhile to note that the rutile based nanorod arrays and the anatase based NP films have different surface properties (e.g. crytal orientation and surface defect concentration,) due to the different crystal structure and morphology, which may affect the adsorption of the dyes and the electron recombination. Lu *et al* have reported that the binding strength between the dye (e.g. N3) and rutile [001] is stronger than the dye with anatase [001].[28] Moreover, Katoh *et al* have found that the distribution of N3 dye on rutile single crystal TiO_2 is homogeneous whereas dye aggregation is found in mesoporous anatase TiO_2 film.[44] Although the information on the adsorption behaviour of the organic dyes on rutile and anatase TiO_2 film is very limited, it is anticipated that the crystal structure of the TiO2 film should have significant influence on adsorption of the organic dyes D205 and C218, and such influence may contribute the electron recombination of the solar cells.

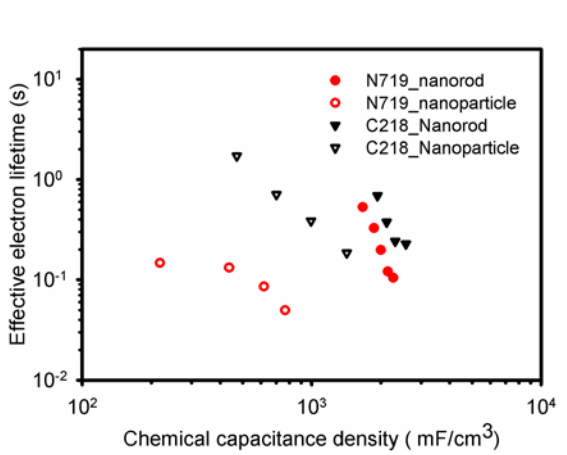

Figure 8. Comparison of the effective electron lifetime of dye-sensitized solar cells with nanorod arrays and mesoporous nanoparticles based films sensitized with N719 and C218

Conclusions

This work has revealed the remarkable characteristic of the dye N719, C218 and D205 in dye-sensitized solar cells using TiO_2 nanorod arrays and the superior performance of the TiO_2 nanorod arrays in reducing the electron recombination compared to conventional nanoparticles based TiO_2 films. The significantly higher light extinction coefficient of the dye C218 results in a 40% higher photocurrent density of the nanorod array based DSSCs compared to the cells with dye N719 and D205. However, the nanorod array based DSSCs coated with N719 (NR-N719) shows a higher open-circuit photovoltage than the cells with the organic dyes. The comprehensive investigation of the electron recombination has disclosed that the higher voltage is originated from the more negative energy level of the conduction band of the TiO_2 film after adsorbed with N719. The effective electron lifetime, τ_n, of the nanorod array based DSSCs with the different dyes shows the trend of C218 > D205 > N719.

Comparison of the effective electron lifetime of the DSSCs with the nanorod arrays (NR) with that of the conventional nanoparticles based TiO_2 films (NP) has confirmed that the nanorod array can significantly improve the electron lifetime, but the beneficial extent is affected by the nature of the adsorbed dye. The τ_n of the NR-N719 is more than two orders of magnitude higher that of the NP-N719 whereas the τ_n of the NR-C218 is only around one order of magnitude higher than that of NP-C218. This phenomenon is ascribed to the lower electron recombination induced by the dye C218 for the DSSCs.

Acknowledgements

The authors (H. Wang and M. Liu) appreciate the financial support from Queensland University of Technology *via* Vice-Chancellor Research Fellowship scheme.

Supporting Information Available: Molecule structure of the dye N719, C218 and D205 and the I-V plots of dye-sensitized solar cells with nanoparticals based TiO_2 films sensitized with N719 and C218 respectively are provided. This material is available free of charge *via* the Internet at http://pubs.acs.org.

References

1. B. Oregan and M. Gratzel, *Nature*, 1991, **353**, 737.
2. M. Gratzel, *Acc. Chem. Res.*, 2009, **42**, 1788.
3. H. X. Wang, H. Li, B. F. Xue, Z. X. Wang, Q. B. Meng and L. Q. Chen, *J. Am. Chem. Soc.*, 2005, **127**, 6394.
4. A. Hagfeldt, G. Boschloo, L. Sun, L. Kloo and H. Pettersson, *Chem. Rev.*, 2010, 110, 6595.
5. H. X. Wang, J. Bell, J. Desilvestro, M. Bertoz and G. Evans, *J. Phys. Chem. C*, 2007, **111**, 15125.
6. S. A. Haque, E. Palomares, B. M. Cho, A. N. M. Green, N. Hirata, D. R. Klug and J. R. Durrant, *J. Am. Chem. Soc.*, 2005, **127**, 3456.
7. T. T. O. Nguyen, L. M. Peter and H. X. Wang, *J. Phys. Chem. C*, 2009, **113**, 8532.
8. L. M. Peter, *J. Phys. Chem. C*, 2007, **111**, 6601.
9. J. Bisquert, D. Cahen, G. Hodes, S. Ruhle and A. Zaban, *J. Phys. Chem. B*, 2004, **108**, 8106.
10. J. Bisquert and V. S. Vikhrenko, *J. Phys. Chem. B*, 2004, **108**, 2313.
11. F. Sauvage, D. H. Chen, P. Comte, F. Z. Huang, L. P. Heiniger, Y. B. Cheng, R. A. Caruso and M. Graetzel, *ACS Nano*, 2010, **4**, 4420.
12. M. Adachi, Y. Murata, J. Takao, J. T. Jiu, M. Sakamoto and F. M. Wang, *J. Am. Chem. Soc.*, 2004, **126**, 14943.
13. E. Ghadiri, N. Taghavinia, S. M. Zakeeruddin, M. Grätzel and J.-E. Moser, *Nano Lett.*, 2010, **10**, 1632.
14. Y. C. Qiu, W. Chen and S. H. Yang, *Angew Chem Int Edit*, 2010, **49**, 3675.
15. F. Sauvage, F. Di Fonzo, A. L. Bassi, C. S. Casari, V. Russo, G. Divitini, C. Ducati, C. E. Bottani, P. Comte and M. Graetzel, *Nano Lett.*, 2010, **10**, 2562.
16. K. Shankar, J. Bandara, M. Paulose, H. Wietasch, O. K. Varghese, G. K. Mor, T. J. LaTempa, M. Thelakkat and C. A. Grimes, *Nano Lett.*, 2008, **8**, 1654.
17. A. C. Fisher, L. M. Peter, E. A. Ponomarev, A. B. Walker and K. G. U. Wijayantha, *J. Phys. Chem. B*, 2000, **104**, 949.
18. L. M. Peter, A. B. Walker, G. Boschloo and A. Hagfeldt, *J. Phys. Chem. B*, 2006, **110**, 13694.
19. S. H. Kang, M. S. Kang, S. H. Choi, J. Y. Kim, H. S. Kim, T. Hyeon and Y. E. Sung, *Electrochem Commun*, 2008, **10**, 1326.
20. M. Paulose, K. Shankar, O. K. Varghese, G. K. Mor and C. A. Grimes, *J. Phys. D-Appl. Phys.*, 2006, **39**, 2498.
21. J. R. Jennings, A. Ghicov, L. M. Peter, P. Schmuki and A. B. Walker, *J. Am. Chem. Soc.*, 2008, **130**, 13364.
22. K. Zhu, N. R. Neale, A. Miedaner and A. J. Frank, *Nano Lett.*, 2007, **7**, 69.
23. B. Liu and E. S. Aydil, *J. Am. Chem. Soc.*, 2009, **131**, 3985.
24. X. J. Feng, K. Shankar, O. K. Varghese, M. Paulose, T. J. Latempa and C. A. Grimes, *Nano Lett.*, 2008, **8**, 3781.
25. M. N. Liu, H. X. Wang, C. Yan, G. Will and J. Bell, *Appl. Phys. Lett.*, 2011, **98**, 133113.
26. J. H. Bang and P. V. Kamat, *Adv. Funct. Mater.*, 2010, **20**, 1970.
27. Z. Ning, Y. Fu and H. Tian, *Energy Environ. Sci.*, 2010, **3**, 1170.
28. Y. F. Lu, D. J. Choi, J. Nelson, O. B. Yang and B. A. Parkinson, *J. Electrochem. Soc.*, 2006, **153**, E131.
29. H. Wang and L. M. Peter, *J. Phys. Chem. C*, 2009, 18125.
30. F. Fabregat-Santiago, J. Bisquert, G. Garcia-Belmonte, G. Boschloo and A. Hagfeldt, *Sol. Energ Mat. Sol. Cells*, 2005, **87**, 117.
31. H. X. Wang and L. A. Peter, *J. Phys. Chem. C*, 2009, **113**, 18125.
32. N. Alonso-Vante, *Sol. Energ Mat. Sol. Cells*, 1993, **31**, 509.
33. H. W. Ham and Y. S. Kim, *Thin Solid Films*, 2010, **518**, 6558.
34. R. Z. Li, J. Y. Liu, N. Cai, M. Zhang and P. Wang, *J. Phys. Chem. B*, 2010, **114**, 4461.

35. A. Mishra, M. K. R. Fischer and P. Bauerle, *Angew Chem Int Edit*, 2009, **48**, 2474.
36. M. K. Nazeeruddin, A. Kay, I. Rodicio, R. Humphrybaker, E. Muller, P. Liska, N. Vlachopoulos and M. Gratzel, *J. Am. Chem. Soc.*, 1993, **115**, 6382.
37. J. Bisquert, F. Fabregat-Santiago, I. Mora-Sero, G. Garcia-Belmonte and S. Gimenez, *J. Phys. Chem. C*, 2009, **113**, 17278.
38. P. J. Cameron, L. M. Peter and S. Hore, *J. Phys. Chem. B*, 2005, **109**, 930.
39. J. Bisquert, A. Zaban, M. Greenshtein and I. Mora-Sero, *J. Am. Chem. Soc.*, 2004, **126**, 13550.
40. W. H. Howie, F. Claeyssens, H. Miura and L. M. Peter, *J. Am. Chem. Soc.*, 2008, **130**, 1367.
41. F. De Angelis, S. Fantacci, A. Selloni, M. Gratzel and M. K. Nazeeruddin, *Nano Lett.*, 2007, **7**, 3189.
42. J. N. Clifford, G. Yahioglu, L. R. Milgrom and J. R. Durrant, *Chem. Commun.*, 2002, 1260.
43. N. G. Park, J. van de Lagemaat and A. J. Frank, *J. Phys. Chem. B*, 2000, **104**, 8989.
44. R. Katoh, K. Yaguchi, M. Murai, S. Watanabe and A. Furube, *Chem. Phys. Lett.*, 2010, **497**, 48.